TU Delft

Delft University of Technology

Document Version
Final published version

Licence
CC BY-NC-ND

Citation (APA)
Schrama, F. N. H., Beunder, E. M., Panda, S. K., Visser, H. J., Moosavi-Khoonsari, E., Sietsma, J., Boom, R., & Yang, Y. (2021). Optimal hot metal desulphurisation slag considering iron loss and sulphur removal capacity part I: fundamentals. *Ironmaking and Steelmaking*, *48*(1), 1-13. https://doi.org/10.1080/03019233.2021.1882647

Important note
To cite this publication, please use the final published version (if applicable).
Please check the document version above.

Copyright
In case the licence states “Dutch Copyright Act (Article 25fa)”, this publication was made available Green Open Access via the TU Delft Institutional Repository pursuant to Dutch Copyright Act (Article 25fa, the Taverne amendment). This provision does not affect copyright ownership.
Unless copyright is transferred by contract or statute, it remains with the copyright holder.

Sharing and reuse
Other than for strictly personal use, it is not permitted to download, forward or distribute the text or part of it, without the consent of the author(s) and/or copyright holder(s), unless the work is under an open content license such as Creative Commons.

Takedown policy
Please contact us and provide details if you believe this document breaches copyrights.
We will remove access to the work immediately and investigate your claim.

This work is downloaded from Delft University of Technology.



Ironmaking & Steelmaking

Processes, Products and Applications

ISSN: (Print) (Online) Journal homepage: https://www.tandfonline.com/loi/yirs20

Optimal hot metal desulphurisation slag considering iron loss and sulphur removal capacity part I: fundamentals

Frank N. H. Schrama, Elisabeth M. Beunder, Sourav K. Panda, Hessel-Jan Visser, Elmira Moosavi-Khoonsari, Jilt Sietsma, Rob Boom & Yongxiang Yang

To cite this article: Frank N. H. Schrama, Elisabeth M. Beunder, Sourav K. Panda, Hessel-Jan Visser, Elmira Moosavi-Khoonsari, Jilt Sietsma, Rob Boom & Yongxiang Yang (2021) Optimal hot metal desulphurisation slag considering iron loss and sulphur removal capacity part I: fundamentals, Ironmaking & Steelmaking, 48:1, 1-13, DOI: 10.1080/03019233.2021.1882647

To link to this article: https://doi.org/10.1080/03019233.2021.1882647

© 2021 Tata Steel Nederland Technology BV. Published by Informa UK Limited, trading as Taylor & Francis Group

Published online: 21 Feb 2021.

Submit your article to this journal

Article views: 291

View related articles

View Crossmark data

Citing articles: 1 View citing articles

Full Terms & Conditions of access and use can be found at
https://www.tandfonline.com/action/journalInformation?journalCode=yirs20

IRONMAKING & STEELMAKING
2021, VOL. 48, NO. 1, 1–13
https://doi.org/10.1080/03019233.2021.1882647

The Institute of Materials, Minerals and Mining

Taylor & Francis
Taylor & Francis Group

RESEARCH ARTICLE

OPEN ACCESS Check for updates

Optimal hot metal desulphurisation slag considering iron loss and sulphur removal capacity part I: fundamentals

Frank N. H. Schrama [a,b], Elisabeth M. Beunder [b], Sourav K. Panda[b], Hessel-Jan Visser[b], Elmira Moosavi-Khoonsari[b]*, Jilt Sietsma [a], Rob Boom [a] and Yongxiang Yang [a]

[a]Department of Materials Science and Engineering, Delft University of Technology, Delft, Netherlands; [b]Tata Steel, IJmuiden, Netherlands

ABSTRACT

In hot metal desulphurisation (HMD) the slag will hold the removed sulphur. However, the iron that is lost when the slag is skimmed off, accounts for the highest costs of the HMD process. These iron losses are lower when the slag has a lower viscosity, which can be achieved by changing the slag composition. A lower slag basicity decreases the viscosity of the slag, but also lowers its sulphur removal capacity, therefore optimisation is necessary. In this study, the optimal HMD slag composition is investigated, considering both the sulphur removal capacity and the iron losses. In part I the theory is discussed and in part II the optimal slag is validated with plant data, laboratory experiments and a thermodynamic analysis.

ARTICLE HISTORY
Received 27 November 2020
Accepted 20 January 2021

KEYWORDS
Hot metal desulphurisation; slag; iron loss; sulphide capacity; basicity; viscosity; steelmaking; process optimisation

Introduction

Since the early days of iron- and steelmaking, sulphur is considered as an unwanted impurity that needs to be removed [1]. Although there are various processes in the modern steelmaking chain where sulphur can be removed, a dedicated hot metal desulphurisation (HMD) process between the blast furnace (BF) and converter (or basic oxygen furnace, BOF) remains necessary. The HMD process benefits from the low oxygen activity of the hot metal at that stage of the process chain (before the BOF). Essentially during the HMD process the dissolved sulphur reacts with reagents (typically magnesium and/or lime) to form sulphides that end up in the slag phase. When the slag is removed after reagent injection, the hot metal is desulphurised [2,3].

As the sulphur is only removed by skimming off the sulphur-containing slag, it is essential for the HMD process that the slag contains all formed sulphides. The mass of sulphur that can be removed with a certain slag, is defined as the 'sulphur removal capacity' of the slag. This sulphur removal capacity is different from the thermodynamically defined 'sulphide capacity' (C_S), which was introduced by Fincham and Richardson [4]. In the present work the sulphur removal capacity of the slag is used as the criterion for optimising slag regarding sulphur removal.

The largest costs during the HMD process are the iron losses, iron that is skimmed off together with the slag. Depending on the heat size, typically 500–4000 kg iron (0.5–2.5 wt-% of the total iron) is skimmed off per heat [5,6]. By changing the apparent viscosity of the slag (η_{slag}), the iron losses can be lowered [6–11]. This means that iron losses partly depend on the slag composition.

The aim of this study is to find the optimal slag for the HMD process, which is defined as a slag with an optimal balance between maximising sulphur removal capacity and minimising iron losses. Because the slag composition changes during the process, as reagents are added, the sulphur removal capacity should be sufficient throughout the process. The slag composition that minimises the iron losses should be reached at the end of the process, so the focus here is on the final slag composition. In order to be acceptable for industry, this optimal slag should not lead to health, safety and environmental issues and should not lead to a large increase in costs. In the present paper, part I of this study, the theory behind the sulphur removal capacity, as well as a theoretical study of HMD iron losses, are presented. This part ends with conclusions about the optimal HMD slag, based on theory. In part II of this study [12] the theory is examined and validated with a Monte Carlo simulation using FactSage [13], plant data analysis and laboratory viscosity and melting point experiments with the optimal slag.

Sulphur removal capacity

Desulphurisation process

In Europe and North America, the magnesium-lime co-injection process is the state-of-the-art HMD process. In this process magnesium and lime are injected into the hot metal. Most of the desulphurisation (> 95%) takes place by the reaction between magnesium and sulphur in the bath (reaction 1). The formed MgS ascends to the slag layer and reacts with lime to form CaS (reaction 2). Only a small portion of the dissolved sulphur directly reacts with lime via reaction 3 [2,14,15].

$$[Mg] + [S] = MgS(s) \quad (1)$$

$$MgS(s) + CaO(s) = CaS(s) + MgO(s) \quad (2)$$

$$CaO(s) + [S] = CaS(s) + [O] \quad (3)$$

In these reactions [x] means that element x is dissolved in hot metal and (s) indicates solid. Most of the formed sulphides

CONTACT Frank N. H. Schrama frank.schrama@tatasteeleurope.com Department of Materials Science and Engineering, Delft University of Technology, Mekelweg 2, 2628 CD, Delft, Netherlands; Tata Steel, IJmuiden, Netherlands
*Now works with Aurubis AG, Hamburg, Germany

© 2021 Tata Steel Nederland Technology BV. Published by Informa UK Limited, trading as Taylor & Francis Group
This is an Open Access article distributed under the terms of the Creative Commons Attribution-NonCommercial-NoDerivatives License (http://creativecommons.org/licenses/by-nc-nd/4.0/), which permits non-commercial re-use, distribution, and reproduction in any medium, provided the original work is properly cited, and is not altered, transformed, or built upon in any way.

Table 1. Typical slag compositions for BF carryover slag and HMD slag after reagent injection [6].

	CaO	SiO_2	Al_2O_3	MgO	MnO	TiO_2	K_2O	Na_2O	CaS
BF carryover [wt-%]	38	37	14	8.9	0.14	0.6	0.45	0.32	0.95
HMD final [wt-%]	37	28	11	13	0.11	0.5	0.34	0.25	9.8

and oxides eventually dissolve in the slag, although a substantial part of the CaS remains in a solid fraction [14]. All solid phases have a lower density than the hot metal and end up in the slag. Since both magnesium and sulphur are dissolved in the metal, reaction 1 is a homogeneous reaction, which is fast. Lime remains a solid throughout the process, making reaction 3 a heterogeneous reaction, which is slower. Besides, reaction 3 is further slowed down by surface passivation of the lime particles. The desulphurisation rate in the co-injection process is therefore controlled by reaction 1 [2,3,14,15]. This leads, via reaction 2, to a heterogeneous slag, which is not necessarily in equilibrium with the hot metal with respect to sulphur distribution. Other sulphur removing processes in steelmaking, including the blast furnace (BF), the Kanbara reactor (KR) HMD process and several secondary metallurgy (post BOF) processes, which include the ladle furnace and the vacuum degasser, are dominated by reaction 3. The slag and metal bath are generally in equilibrium regarding the sulphur distribution. Metallic magnesium is not introduced for desulphurisation of the metal in any of the above-mentioned processes [2,3,15–18].

Before the HMD process starts, typically 1–3 t of BF carryover slag floats on top of the hot metal. During the reagent injection CaO, CaS and MgO are added to the slag, contributing to typically 20–40 wt-% of the slag after injection. This means that the slag's composition and properties change during the process. Especially the slag's basicity increases during the injection. Table 1 shows how a typical HMD slag changes from the start of injection (BF carryover slag) until the end of injection (HMD final slag).

As slag compositions can change from plant to plant and heat to heat, Table 2 gives the typical range of HMD slag composition and temperature after reagent injection.

In the slag composition the amount of FeO_x (FeO and Fe_2O_3) has been excluded, as it is difficult to measure the amount of FeO_x in the slag. With XRF (X-ray fluorescence) analysis, which is a typical method for slag analysis, all components are oxidised, so no distinction between FeO_x dissolved in the slag, and metallic Fe, captured in the slag, can be made. FeO_x does have a significant effect on the viscosity and melting point of the slag [17,19]. Figure 1 illustrates the effect of adding FeO to a slag with a balanced composition of 40 wt-% Cao, 30 wt-% SiO_2, 15 wt-% Al_2O_3 and 10 wt-% MgO on the slag's liquidus temperature (T_{liq}) at thermodynamic equilibrium (determined with FactSage 7.3 [20]). The FeO_x concentration in BF carryover slag is typically estimated around 1 wt-%, but can be up to 3 wt-% [15,21,22].

Sulphide capacity

When the oxygen partial pressure (p_{O2}) < 1 Pa (10^{-5} atm), the only way for a sulphur atom to enter the slag is to replace an oxygen atom in an oxide (usually CaO). Under these conditions sulphur is only present in the slag as a sulphide. When $p_{O2} > 100$ Pa (10^{-3} atm), sulphur will be present as sulphate in the slag [4]. It is generally accepted that in HMD p_{O2} is much lower than 10^{-5} atm (in some literature a p_{O2} of 10^{-15} atm. is mentioned [23]), so all sulphur in the slag will be present in the form of sulphides. In this study there is a clear difference between the practical 'sulphur removal capacity' and the thermodynamically defined sulphide capacity (C_S), which was introduced by Fincham and Richardson [4]. Here the sulphur removal capacity is defined as the amount of sulphur that can be removed with a certain slag, not necessarily in equilibrium with the hot metal. C_S is defined as 'the potential capacity of a melt to hold sulphur as a sulphide' [4,24], which is given in Equation (4). It should be noted that the main difference between the sulphur removal capacity and the sulphide capacity is that the sulphide capacity only takes dissolved sulphides in the liquid slag at equilibrium into account, while the sulphur removal capacity also takes solid sulphides, as well as dissolved sulphides that are not in equilibrium into account. Therefore, the sulphur removal capacity of a slag is a better quantity to judge sulphur removal in operational practice since it is typically higher than its sulphide capacity.

$$C_S = X_{(S)}\sqrt{\frac{p_{O2}}{p_{S2}}} \tag{4}$$

Here $X_{(S)}$ is the weight percentage of the sulphides in the slag and p_{O2} and p_{S2} the partial pressures of the oxygen and sulphur, respectively, in the gas phase in equilibrium with the slag. Equation (4) is valid when Henrian behaviour of sulphur in the slag is expected (because of the low solubility) [25]. As C_S is difficult to measure directly, often the sulphur distribution ratio (L_S) is used, which is the ratio between sulphur in the slag ($X_{(S)}$, typically as sulphides) and sulphur dissolved in the hot metal ($X_{[S]}$) [24–26]:

$$L_S = \frac{X_{(S)}}{X_{[S]}} \tag{5}$$

C_S can be calculated based on L_S with Equation (6):

$$\log(C_S) = \log(L_S) + \log(K^{\ominus}_{S2}) - \log(f_S) + \log(a_O) \tag{6}$$

Here f_S is the Henrian sulphur activity coefficient in the hot metal (typically 2.5 [27]), a_O is the oxygen activity of the hot metal and $K^{\ominus}_{S2}$ is the reaction equilibrium constant for the general desulphurisation reaction between sulphur and oxygen (reaction 7). $K^{\ominus}_{S2}$ is calculated with

Table 2. Composition and temperature range for HMD slags after reagent injection.

	CaO	SiO_2	Al_2O_3	MgO	MnO	TiO_2	K_2O	Na_2O	CaS	T [°C]
Min [wt-%]	30	23	6	10	0.03	0.4	0.1	0.08	5	1250
Max [wt-%]	43	33	15	17	0.25	1.2	0.7	0.6	15	1425

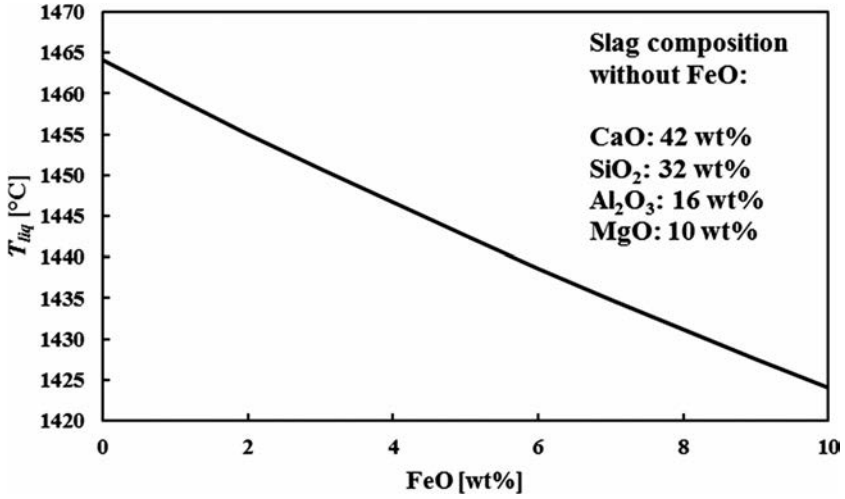

Figure 1. Effect of FeO concentration on T_{liq} in a slag with a balanced composition of 40 wt-% CaO, 30 wt-% SiO_2, 15 wt-% Al_2O_3 and 10 wt-% MgO. Determined with FactSage 7.3.

Equation (8) (T is the temperature in K) [26,28].

$$[S] + \frac{1}{2}O_2(g) = \frac{1}{2}S_2(g) + [O] \tag{7}$$

$$\log\left(K_{S2}^{\Theta}\right) = -\frac{935}{T} + 1.375 \tag{8}$$

Because the BF is a reducing process, a_O of the hot metal is low. In literature different values are mentioned, between $3{\cdot}10^{-6}$ (3 ppm) and $5{\cdot}10^{-7}$ (0.5 ppm). Ender et al. [29] used electromagnetic force (EMF) measurements to determine a_O before and after the HMD process at the ThyssenKrupp steel plant in Duisburg, Germany. Before HMD a_O is typically 1.2–1.6 ppm and after HMD it is 0.7–1.2 ppm. Kitamura [15] mentions an a_O of 2–4 ppm. Zhao and Irons [30] measured an a_O between 0.5 and 1.0 ppm during a laboratory experiment where CaC_2 was added to hot metal. Janke [23] measured a_O values in hot metal between 0.5 and 1.0 ppm as well. In iron foundries a_O values between 0.1 and 0.6 ppm are measured [31,32]. These differences in a_O are caused by different process conditions, the large error for EMF measurements at low ranges and typical HMD temperatures (up to 50% [29]) and the different measurement depth. It is expected that a_O at 50 cm below the metal-slag interface, where industrial EMF measurements are typically done, is higher than at the metal-slag interface itself, where carbon oversaturation and precipitation locally lowers a_O [14,33]. As for C_S the a_O value at the metal-slag interface is relevant, $a_O = 5{\cdot}10^{-7}$ (0.5 ppm) is used in this study.

The combination of Equations (6) and (8) gives the impression that for a certain slag composition C_S only depends on temperature. Panda et al. [26] showed with FactSage calculations with a private database (CON2) for typical ladle furnace slags, that this is true only at high p_{O2} values (for ladle furnace slags typically $p_{O2} > 0.1$ Pa), or low p_{S2} values (typically $p_{S2} < 1$ Pa). At lower p_{O2} or higher p_{S2} values, p_{O2} and p_{S2} will influence C_S. Jung and Moosavi-Khoonsari [34] stated that the concept of C_S, where the amount of sulphides that a slag can contain only depends on its composition and temperature, is only valid if the slag contains a low fraction of sulphides. If the slag contains more sulphides, p_{O2} and p_{S2} play a role as well. This means that for processes where relatively low amounts of sulphur need to dissolve in the slag, like desulphurisation in secondary metallurgy, C_S is a unique temperature- and composition-dependent property of the slag. In HMD, the slag contains more sulphides (HMD slag can contain up to 15 wt-% CaS), which means that C_S under HMD conditions is a function of p_{O2} and p_{S2} as well.

In literature, many authors made a model to predict C_S based on the slag composition, often including the optical basicity (Λ), which was defined by Duffy and Ingram [35] as:

$$\Lambda = X_1\Lambda_1 + X_2\Lambda_2 + \ldots \tag{9}$$

where X_n is the weight percentage of component n and Λ_n is the optical basicity value for component n. In this work Λ is

Table 3. Overview of different models to determine C_S, based on optical basicity (Λ). T is in K.

Authors	Model for $\log(C_S)$	Eq.	Reference
Hao & Wang *	$19.45 - \frac{11.85}{\Lambda_{corr}} + \frac{\frac{12\,410}{\Lambda_{corr}} - 27\,109}{T}$	(10)	[41]
Shankar et al.	$\log\left(-9.852 \cdot 10^{-6} \cdot X_{Al2O3} + 0.010574\Lambda - \frac{16.2933}{T} + 0.002401\right)$	(11)	[42]
Sosinsky & Sommerville	$\frac{22\,690 - 54\,640\Lambda}{T} + 43.6\Lambda - 25.2$	(12)	[43]
Young et al.	$-13.913 + 42.84\Lambda - 23.82\Lambda^2 - \frac{11\,710}{T} - 0.02223X_{SiO2} - 0.02275X_{Al2O3}$	(13)	[36, 37]
Zhang et al.	$-6.08 + \frac{4.49}{\Lambda} + \frac{15\,893 - \frac{15\,864}{\Lambda}}{T}$	(14)	[44]

*Hao and Wang used an alternative Λ: Λ_{corr}, which differs for HMD slag 10-13% from Λ.

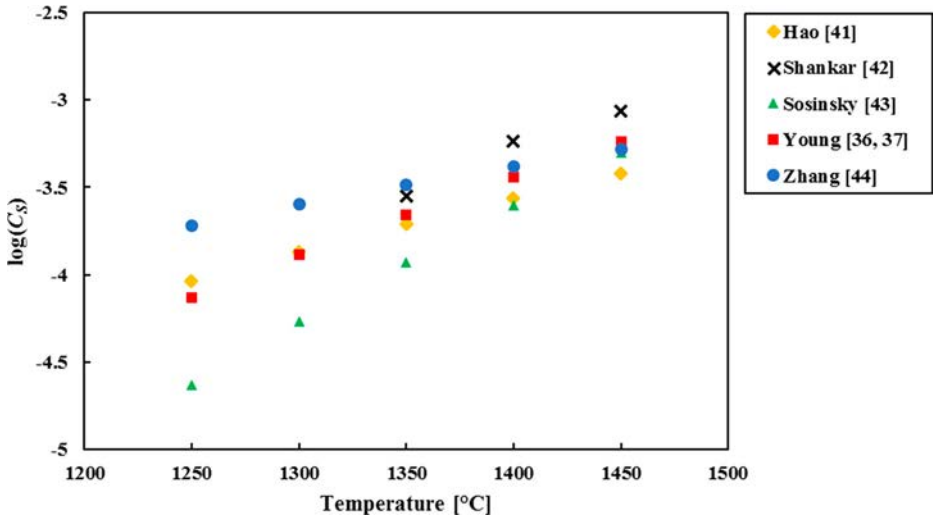

Figure 2. Comparison of C_S determined by the models from Table 3, for different temperatures.

determined with only the main components of the slag (normalised to 100%): CaO ($\Lambda_{CaO} = 0.01$), MgO ($\Lambda_{MgO} = 0.0078$), SiO_2 ($\Lambda_{SiO2} = 0.0048$) and Al_2O_3 ($\Lambda_{Al2O3} = 0.006$) [36,37]. Leaving out the minor slag components does not lead to significant differences in Λ.

Ma et al. [38] made an overview of different models to predict C_S, based on the slag composition and Λ. Table 3 gives an overview of the models for $log(C_S)$. The KTH model [39] is excluded from this list, because it gave an opposite trend when changing the MgO content. Also the model of Taniguchi et al. [40] is excluded, because it is developed for a steel slag composition range, which made it too sensitive for MgO values above 10 wt-%, making it not valid for the HMD slag range.

The two most influential factors for C_S are temperature and, via Λ, CaO content. Figures 2 and 3 show the influence of temperature and CaO, respectively, on the C_S determined by the models from Table 3. A simplified typical HMD slag composition was used (40 wt-% CaO, 35 wt-% SiO_2, 9 wt-% MgO, 16 wt-% Al_2O_3; when changing the CaO concentration the other components were changed in the same ratio).

Although the different models give different outcomes for a typical simplified HMD slag, the $log(C_S)$ value ranges from −3 to −5, also when the temperature or the CaO content is changed within relevant ranges. Condo et al. [45] measured C_S for synthetic typical BF slags, which are comparable to HMD slags in composition, temperature and p_{O2}, and they also found $log(C_S)$ values around −4.

C_S in an industrial HMD

To understand the significance of C_S for the HMD process, the apparent C_S is determined for industrial HMD heats. At the industrial HMD process, all sulphur that is removed from the hot metal ends up in the slag. Therefore, when the initial and final sulphur content of the hot metal at the HMD is known and an estimate for the slag weight is made (assuming 1500 kg carryover slag from the BF for a typical heat size of 300 t), L_S can be calculated for every heat. When assuming typical values for $f_S = 2.5$ and $a_O = 5{\cdot}10^{-7}$, C_S can be calculated for every heat with Equation (6). Furthermore, the final composition of the slag can be estimated for every heat by assuming an average BF carryover slag composition and adding the injected reagents to that slag, assuming that all removed sulphur in the slag is CaS. Also, a homogeneous slag is assumed. Figure 4 gives the $log(C_S)$ values of 47,129 HMD heats from Tata Steel, IJmuiden, set against the $log(C_S)$ values predicted by Young's model (Equation (13)) based on the slag composition and temperature.

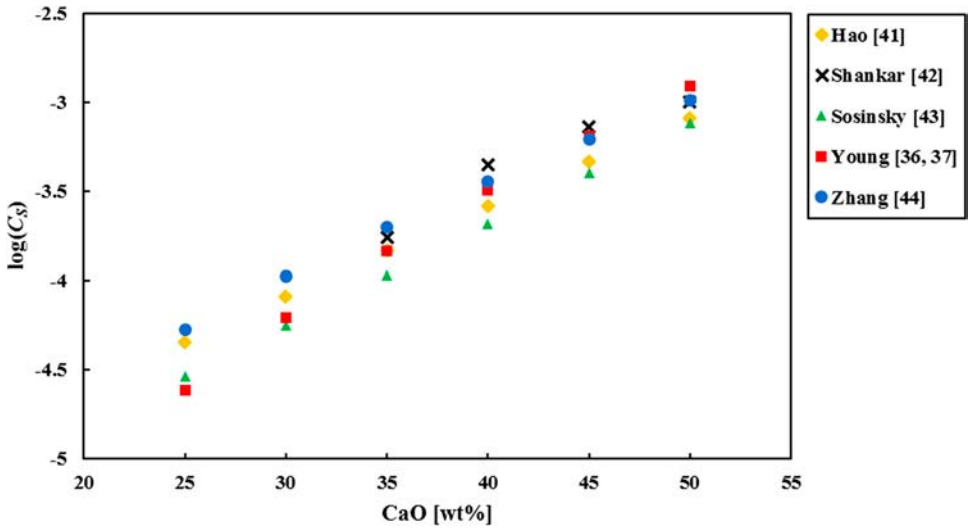

Figure 3. Comparison of C_S determined by the models from Table 3, for different CaO concentrations at 1400°C.

The accuracy of the method to determine C_S for a single industrial heat is not very high, because of the rough assumptions made. When applying this method to more than 47 thousand industrial heats, the order of magnitude of the C_S values is the same, but the variation cannot be described by Young's model. It is clear that, despite of the scatter, Young's model predicts the C_S values based on plant data quite well. Young's model showed the best correlation with the plant data compared to the other models from Table 3. It seems that desulphurisation of hot metal can be predicted by the slag composition (translated to Λ) and temperature only. It has to be noted that when an a_O of 3 ppm is used, instead of the 0.5 ppm which is used in the present work, Young's model (and the other models from Table 3) underestimate C_S by a factor 10. The actual C_S greatly depends on a_O. Therefore, models based on slag composition (or Λ) rely on the assumption that slag and hot metal are in equilibrium.

Most of the desulphurisation in the magnesium-lime co-injection HMD process takes place in the hot metal itself via reaction (1), as this reaction is much faster than reaction (3). The composition of the slag has no influence on the reaction with Mg. Only reactions (2) and (3) take place at the hot metal-slag interface (at least for a large part). If reaction (1) is significantly faster than reaction (2), the slag and hot metal will not be at equilibrium. Since almost no MgS can be found in industrial HMD slag [14], all MgS that is formed via reaction (1) will react to CaS via reaction (2) during the HMD process. Furthermore, resulphurisation (sulphur from the slag dissolving again in the hot metal) is observed in industry, but this is in the order of magnitude of 1–10 ppm. If the metal and slag were far from equilibrium, larger resulphurisation would be observed in industry, especially for heats that are delayed between HMD and BOF. Magnelöv et al. [7] stated that C_S calculated based on Λ is not applicable for the HMD process, because the HMD slag is not homogeneous and fully liquid. This inhomogeneity of the slag is another explanation for the large scatter in Figure 4.

Table 4. Influence of slag components and temperature on C_S, ranging from ▼ (negative) to ▲▲ (very positive).

Component	Effect	Source	Comment
CaO	▲▲	[3,10,40,46,47]	
SiO_2	▼	[3,25,40,47]	
Al_2O_3	▼	[3,25,46]	
MgO	0	[25,40]	
MnO	▲	[26,40]	No effect above 10%
Na_2O	▲	[48]	
K_2O	▲	[20]	
FeO_n	▼	[20]	
CaF_2	▼	[49]	
Temperature	▲	[3,10,25,26,28,40,46]	

The plant data shows that for individual heats a C_S prediction can be a factor 10 off from the actual desulphurisation. This is because of practical constraints, like measurement errors, slag inhomogeneity and non-dissolved CaS. Therefore, a C_S prediction model is not sufficiently accurate for industrial use at the HMD process. However, C_S can be used to determine the optimal slag composition. Table 4 gives the influence of different slag components and temperature on C_S based on a literature study.

It should be noted that the effect of MgO is marginal. Under industrial conditions it has a slight positive effect as it often replaces C_S-negative components like SiO_2 or Al_2O_3. Note that in this table the slag component MgO is discussed and not the metallic Mg, which is injected during the HMD process to desulphurise the hot metal.

Basicity

The C_S depends on the basicity of the slag, which depends on the slag composition. Understanding basicity as having a high concentration of free oxygen, which can be replaced by sulphur more easily, helps understanding that slags with a higher basicity will pick up more sulphur and thus help desulphurisation. This explains the large influence of a_O on

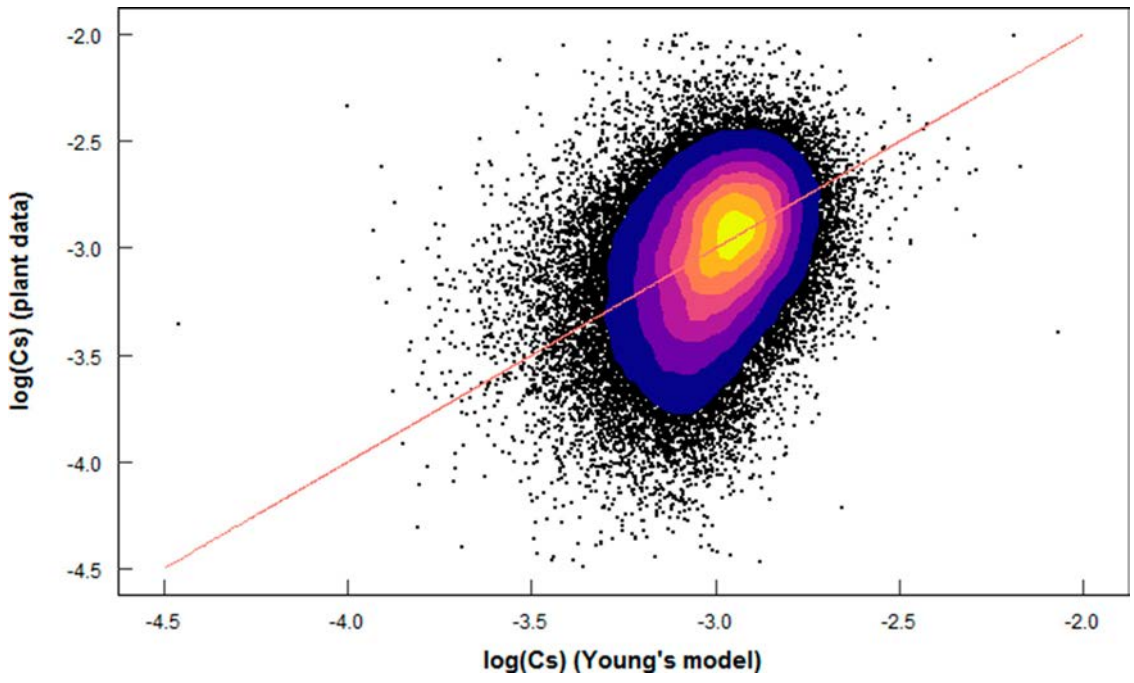

Figure 4. Density plot of $log(C_S)$ values for 47,129 heats at the Tata Steel IJmuiden HMD stations, where the predicted values from Young's model are on the *X*-axis and the actual values based on removed sulphur are on the *Y*-axis.

C_S as well. There is no universal quantitative definition of basicity available. Therefore, different empirical definitions are used today, including optical basicity Λ (defined by Young et al. [36,37]) and the CaO/SiO_2 (known as *B2*) ratio (which can be extended with MgO, Al_2O_3 and P_2O_5), which is commonly used in steel plants [50,51].

Although basicity is hard to quantify from a scientific point of view, an empirical definition of the basicity, like *B2*, is sufficient for industrial practice. In a slag with a basicity (*B2*) below 0.93, which is equal to a molar ratio $CaO:SiO_2$ of 1:1, the CaS formation will be retarded by the lack of free oxygen (O^{2-} ions), which are donated by basic oxides. For completeness MgO (as O^{2-} donator) and Al_2O_3 (which can act as O^{2-} acceptor) should also be taken into consideration [3,34,50]. Above this minimum slag basicity, there should be enough CaO, stoichiometrically, to react with the MgS, according to reaction (2) (MgS reacting to CaS). Only kinetics (like undissolved lime not being in contact with the hot metal, for example the core of a lime particle [2]) will hamper this reaction. Therefore, in industry some extra lime will be needed on top of the lime required to bring the *B2* above 0.93 and the lime required for reaction (2). How much extra lime is required is difficult to quantify on a theoretical basis. Li et al. [52] suggest a minimum *B2* of 1.1, based on industrial experience.

Iron loss

Types of iron loss

The definition of iron losses during the HMD process is the amount of Fe that is (unwantedly) removed during the HMD process (mostly during the skimming). Iron losses can mount up to 0.5–2.5% of the total hot metal weight. The total iron losses depend on the ladle size and geometry, larger ladles typically lead to lower iron losses, but also on the slag conditions and the skimming skills of the operator [5–10,22,52,53]. It is hard though to have an accurate number for iron losses (via slag), since the iron distribution in the slag is not homogeneous, so a sample will not give an accurate value [22,53]. Also determining the iron loss by measuring the weight difference before and after skimming is inaccurate by a few hundred kilograms (approximately 5 wt-% of the slag), as the amount of BF carryover slag that was present is unknown and the weight measurements themselves are inaccurate, which makes an accurate mass balance under industrial conditions not possible. There are different types of iron losses:

- Colloid loss: iron droplets entrapped in the slag in colloidal form (like an emulsion) and removed together with the slag (see Figure 5).
- Entrainment loss: iron entrained with the slag during skimming (see Figure 5).
- Dust loss: iron that leaves the system as dust.
- Skull formation: iron that solidifies at the ladle rim or skimmer paddle and forms skull.
- Chemical loss: iron that reacts and ends up in the slag.

Of these types colloid loss and entrainment loss are the most important. Together they cover > 95% of the total iron loss. SEM analysis of industrial HMD slag, done by Yang et al. [53, 54], shows both small (< 0.5 mm) round iron droplets, typical for colloid loss, and large (> 0.5 mm) irregular shaped iron, typical for entrainment loss. The total amount of iron of both droplet types is in the same order of magnitude. Although this method makes it difficult to exactly quantify the size of colloid loss and entrainment loss, it does prove that both types of iron loss are of comparable size.

Colloid loss (also referred to as emulsion loss) is the most frequently described type of iron loss in HMD. According to literature [6–10,53–56] different factors (in terms of slag chemistry) contribute to the colloid loss:

- Viscosity of the slag: a higher viscosity leads to higher iron losses.
- Solid fraction: more solids in the slag lead to higher iron losses. A higher solid fraction also increases the slag's viscosity.
- Particle size and shape of the solids in the slag: bigger and variable sized particles lead to higher iron losses.
- Interfacial tension and wettability: a lower interfacial tension between slag and iron leads to higher iron losses.
- Iron droplet size: smaller iron droplets lead to higher iron losses

Entrainment loss is difficult to measure. Even if the total iron loss could be measured accurately, it is difficult to distinguish clearly between entrainment loss and colloid loss afterwards. Operators claim that the more viscous and sticky a slag is, and the more solid pieces it contains, the easier it is to skim. They estimate lower entrainment losses

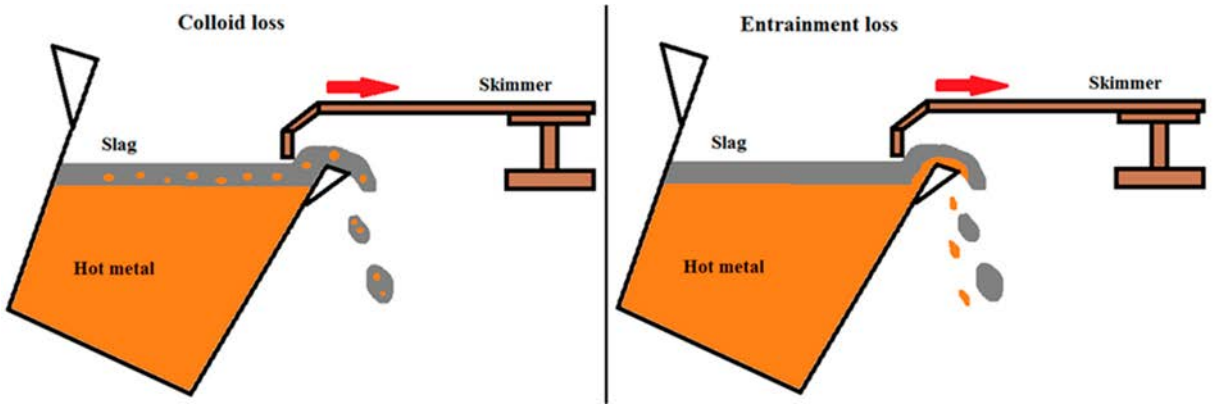

Figure 5. Schematic representation of colloid loss (left) and entrainment loss (right) during skimming in the HMD process [6].

under these conditions. However, plant data show that iron losses increase at higher viscosities. It seems that the increased colloid losses have a larger effect on the total iron losses than the decreased entrainment losses when the slag is more viscous. In industry, entrainment loss is often minimised by mechanical improvements, like increasing the accuracy of the skimmer control or cleaning the skimmer paddle more often, or by operator training, rather than changing the slag properties.

Slag properties will not have major influence on **dust loss** and **skull formation**. Samples at the dust filters of the HMD station show that typically 0.01 % of the iron is lost via the dust (10–30 kg per heat). Skull formation is estimated to be 5–10 kg per heat. Both dust loss and skull formation contribute only little to the total iron losses.

Chemical loss is a hypothetical type of iron loss. It is possible that Fe from the hot metal reacts, most likely with oxygen, and ends up in the slag. Although most iron in the slag is in its metallic form, there is also FeO_x present. From the FeO_x in the slag it is impossible to determine when and how it was formed, as BF carryover slag already contains some FeO_x. Based on the low amount of FeO_x in the HMD slag (typically 1–3 wt-%) and the small exposure of the hot metal to oxygen, it is expected that the contribution of chemical loss to the total iron loss is negligible. Besides, the only way to prevent oxygen from the air to react with the hot metal would be to keep it constantly under inert conditions, which is not a viable solution in industry.

Iron droplets

Changing the slag viscosity has a larger influence on the colloid loss than on the entrainment loss. Therefore, when trying to influence the iron losses via the slag properties, which is the scope of this research, the focus should be on the colloid loss. The iron droplets, present in the slag in colloidal form, do not have a uniform size and shape. Their size and shape depends on the way the droplets are formed. Two mechanisms of how iron droplets are formed are described in literature (see Figure 6). In mechanism I, droplets are formed by iron being entrained by N_2 and Mg gas into the slag, where they will get a regular round or oval shape to minimise the surface area. In mechanism II droplets are formed by iron being splashed through the open eye on top of the slag, where it solidifies in an irregular shape [9,53,54]. Han and Holappa [57] showed with hot metal experiments that droplets formed via mechanism I are not spherical, but irregularly shaped (in the experiments most droplets had a diameter, d_{drop} < 10 µm). The droplets do become spherical when solidifying. Besides, they define two separate mechanisms within mechanism I: film entrainment and bubble entrainment of the iron.

Yang et al. [53] found that when the injection process lasts longer, more iron ends up in the slag via mechanism I (there is an almost linear relationship), while the amount of iron in the slag via mechanism II hardly depends on the injection time at all. This is in contradiction with what Visser [14] suggested, that iron in the slag builds up over time via mechanism II. However, Visser did not consider mechanism I as a significant source of iron and did not investigate both mechanisms. Yang and Visser agree that the total amount of iron in the slag does increase when the injection process lasts longer.

Viscosity of the slag

It is generally accepted that a lower apparent slag viscosity (η_{slag}) leads to lower colloid losses, which usually also leads to lower overall iron losses. Figure 7 shows the estimated iron loss per heat (300 t) for 47,109 heats at the HMD stations at Tata Steel, IJmuiden, for the estimated η_{slag}.

The η_{slag} (in Pa·s) is estimated based on the Einstein-Roscoe equation [58] (Equation (15)), which can be used to determine η_{slag} for slags.

$$\eta_{slag} = \eta_0 \cdot (1 - \varphi_{s,slag} \cdot \alpha)^{-n} \tag{15}$$

Here η_0 is the viscosity of the liquid part of the slag, $\varphi_{s,slag}$ is the volume fraction of solids in the slag, α and n are empirical constants. Assuming that the solid particles are spherical and of uniform size, typically $\alpha = 0.8$ and $n = 2.5$ (these values vary with temperature).

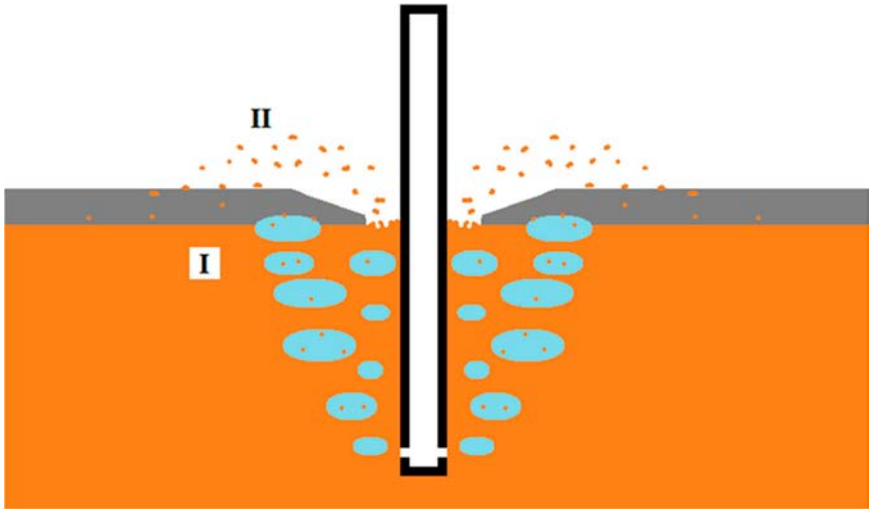

Figure 6. Schematic representation of iron droplet formation mechanisms at HMD. Mechanism I shows droplets entrained by gas bubbles; mechanism II shows droplets launched from the slag eye on top of the slag.

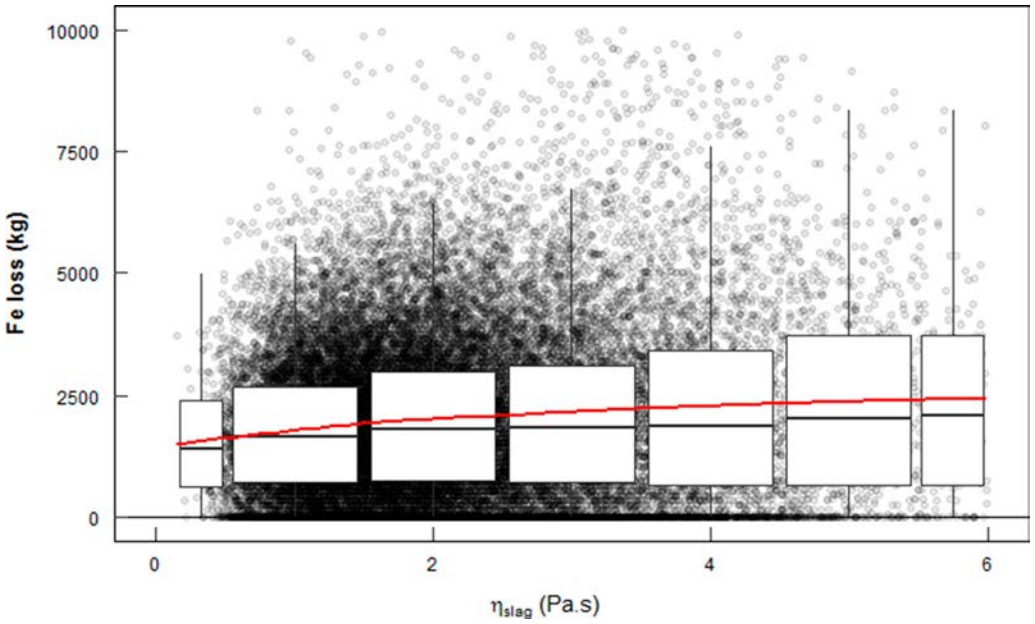

Figure 7. Iron loss at different ηslag at Tata Steel in IJmuiden. Circles show the individual heats. The boxes stretch from the 25th till the 75th percentile of the distribution. The lines (whiskers) extend to 1.5 times the interquartile range. In red a polynomial trendline.

To determine η_0 and $\varphi_{s,slag}$, simplified equations, based on FactSage calculations, were used. These equations depend on temperature and on the fractions of the major slag components (CaO, SiO_2, Al_2O_3, MgO and CaS), where the temperature has the largest influence on both η_0 and $\varphi_{s,slag}$. The slag composition is estimated by taking an average BF carryover slag composition and adding the injected reagents and removed sulphur, assuming that all sulphur becomes CaS and all Mg becomes MgO. The iron loss is estimated by doing a mass balance over every heat, measuring the ladle weight before and after the HMD process and estimating the BF carryover slag (typically 1500 kg) and the amount of slag that remains in the ladle after skimming (typically 500 kg). The method to estimate η_{slag} and iron loss is inaccurate. Estimating viscosities of industrial slags always leads to large errors, typically $> \pm 30$ % [59]. However, the large amount of data (47 109 heats) makes the trend reliable. It is clear that a higher η_{slag} leads to higher iron losses.

With the help of Stoke's law (Equation (16)) the influence of η_{slag} on the time an iron droplet needs to settle back from the slag into the metal bath, can be estimated [14,55].

$$v_{drop} = \frac{g \cdot d_{drop}^2 \cdot (\rho_{HM} - \rho_{slag})}{18 \cdot \eta_{slag}} \tag{16}$$

Here v_{drop} is the settling speed (m/s) of the iron droplet, d_{drop} is the droplet's diameter (m), g is the gravity constant (9.81 m s^{-2}) and ρ_X is the density of hot metal (HM) or slag (kg·m^{-3}). Typically, ρ_{HM} is 7000 kg·m^{-3}, ρ_{slag} is around 2 700 kg m^{-3}, iron droplets in the slag have diameters between 0.01 and 10 mm and η_{slag} can vary between 0.9 and 20 Pa·s [14]. For d_{drop} > 0.1 mm, v_{drop} can better be determined with the Hadamard–Rybczynski equation,

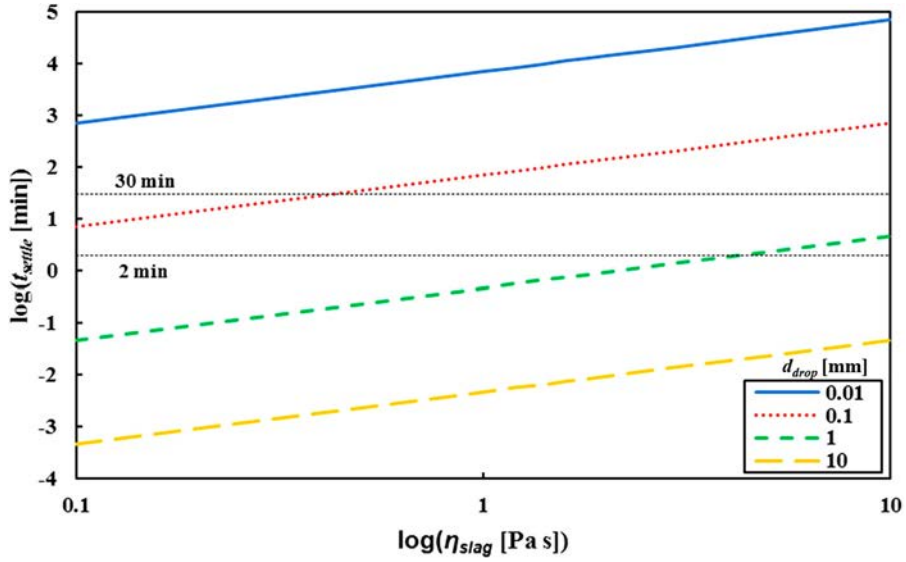

Figure 8. The influence of η_{slag} on t_{settle} for different d_{drop} (ranging from 0.01 to 10 mm) with h_{slag} = 10 cm.

which neglects the surface tension of the droplet [55]:

$$v_{drop} = \frac{g \cdot d_{drop}^2 \cdot (\rho_{HM} - \rho_{slag})}{12 \cdot \eta_{slag}} \quad (17)$$

Figure 8 shows the influence of η_{slag} on the settling time (t_{settle}) of iron droplets with a d_{drop} of 0.01–10 mm in a slag with a thickness (h_{slag}) of 10 cm, which is typical for HMD slag [14, 53, 54]. Equations (16) and (17) were used to determine v_{drop}.

Under industrial conditions, the minimum time between stop reagent injection and start skimming is 2 min (lance lifting, sampling and ladle tilting). Droplets that settle in less than 2 min will therefore never be skimmed off. Under normal conditions, the maximum time between the start of reagent injection and the end of skimming is 30 min. Droplets that take more than 30 min to settle will always be removed together with the slag, if they start on top of the slag. For droplets with a settling time between 2 and 30 min, it depends on the moment they ended up in the slag and on the moment when the skimming starts, whether they are skimmed off or not. Note that the mentioned settling times are valid for a droplet that starts on top of the slag; for droplets that end up in the slag via mechanism I and start at a lower point in the slag, different settling times apply. In this simplified model, the extra friction for droplets that are not spherical, as well as the surface tension a droplet has to overcome when it lands on top of the slag, has been neglected.

Nevertheless Figure 8 shows that, regardless of the circumstances, droplets with $d_{drop} > 2$ mm will always settle before skimming starts. Droplets with $d_{drop} < 0.5$ mm will never settle in time. This means that by optimising η_{slag} and the allowed t_{settle}, within industrial boundaries, only the droplets between 0.5 and 2 mm can be retrieved.

Temperature has the largest influence on η_{slag}, but the temperature is already maximised in most steel plants, to save energy and to allow more scrap addition in the converter. Slag composition also influences η_{slag}, although the impact is lower. Different slag components will influence η_{slag}, according to Einstein-Roscoe, by changing the liquidus temperature (T_{liq}) and thus $\varphi_{s,slag}$, or by changing η_0. The influence of many slag components on T_{liq} and η_0 has been studied by many authors before. Table 5 gives an overview of the influence of the most common slag components on T_{liq} and η_0 under typical HMD conditions. As the influence of slag composition on T_{liq} and η_0 is complex, the given directions in the table are not universal.

Although many components are able to lower T_{liq} and η_0 of the slag, some of them have disadvantages that make them unwanted or restricted for an optimal slag. Halogen-based components (CaF_2, $CaCl_2$) are harmful for human health and environment. Besides, fluoride-based components lower the desulphurisation efficiency of magnesium [6]. Adding too much alkali metal oxides (Na_2O and K_2O), will make the slag less suitable for recycling at the BF, as alkali metals tend to recirculate inside the BF due to their low boiling point, which leads to an unwanted build-up of these elements [16,17]. Furthermore, TiO_2 leads to Ti(C,N) formation. Ti(C,N) particles form a layer between the slag and hot metal and make the slag sticky, resulting in higher iron losses [14,64]. Finally, the fact that SiO_2 lowers T_{liq}, but increases η_0, while CaO does the opposite, explains some typical misunderstandings in steelmaking regarding the influence of basicity on η_{slag}. Einstein-Roscoe's equation (Equation (15)) shows that for lower temperatures, where part of the slag is solid, lowering the solid fraction by lowering T_{liq}, lowers η_{slag}. At higher temperatures, where the slag is fully liquid, only lowering η_0 will lower η_{slag}. In secondary metallurgy, slag temperatures are high (> 1500 °C) and the slags are usually liquid. Under these conditions a higher basicity decreases η_{slag}. As HMD slag has lower temperatures, typically part of the slag is solid, so a lower basicity (more SiO_2) decreases η_{slag}.

Table 5. Influence of different slag components on T_{liq} and η_0, under typical HMD conditions.

Component	T_{liq}	η_0	Source	Comment
CaO	▲▲	▼	[10,20,60,61]	η_{slag} will go up with CaO
SiO_2	▼	▲	[20,52,60]	
Al_2O_3	▼	▼	[19,60,62]	Below 10 % η_0 ▲ [19]
MgO	▲▲	▼	[20,52,60,62]	
TiO_2	▼	▼	[20,48,63]	
Na_2O	▼	▼	[20,48,52,60]	Below 3 % T_{liq} ▲ [60]
K_2O	▼	▼	[20,49,60]	
MnO	▼	▼	[20]	
CaF_2	▼▼	▼	[6,20,49,56]	
$CaCl_2$	▼	▼	[62]	
FeO_x	▼	▼	[19,20]	
T	na	▼	[20]	

Solid fraction of the slag

It is generally accepted that a lower solid fraction of the slag leads to lower iron losses. Although a fully liquid slag will lead to increased entrainment losses, the decrease in colloid losses will more than make up for that. Industrial data showed that higher temperatures, resulting in a higher liquid fraction of the slag, lead to lower overall iron losses [10]. It should be noted that a substantial amount of the CaS will not dissolve in the HMD slag and, as it has a melting point of 2525 °C, will remain as a solid in the slag.

As the HMD slag is not a homogeneous single phase, the slag will not have a single melting point. Therefore, typically part of the slag is solid, while another part is liquid. The larger the liquid part of the slag is, the lower the iron losses are [4,11,52]. In order to better understand the influence of the slag composition on the liquid fraction of the slag, the slag can be viewed at as if it is homogeneous. With the thermodynamic software FactSage, using a private database [13,20], a ternary diagram is made to show T_{liq} for CaO–SiO_2–Al_2O_3 slag with 10 wt-% MgO (typical for HMD slags), which is shown in Figure 9.

It should be noted that the other slag components all lower T_{liq}, as can be seen in Table 5. Therefore at the BF and HMD the actual T_{liq} will be lower than expected based on Figure 9. When keeping the HMD slag composition range from Table 2 in mind, it is clear that lowering the slag's basicity, so adding more SiO_2 and Al_2O_3, would lower T_{liq} of the slag. It is remarkable that the composition of BF carryover slag is closer to the 'sweet spot' with the lowest T_{liq} than the HMD slag composition after injection. This is due to the fact that at the BF a liquid slag is favourable and therefore a control target [16,17]. During the HMD process effectively MgO (via reactions 1 and 2) and CaO, which both increase T_{liq}, are added to the slag.

In literature MgO, CaO/SiO_2 (*B2*) and Al_2O_3 (together with FeO_x) are identified as the components with the largest influence on T_{liq} of HMD slag [52,60,62]. Li et al. [60]

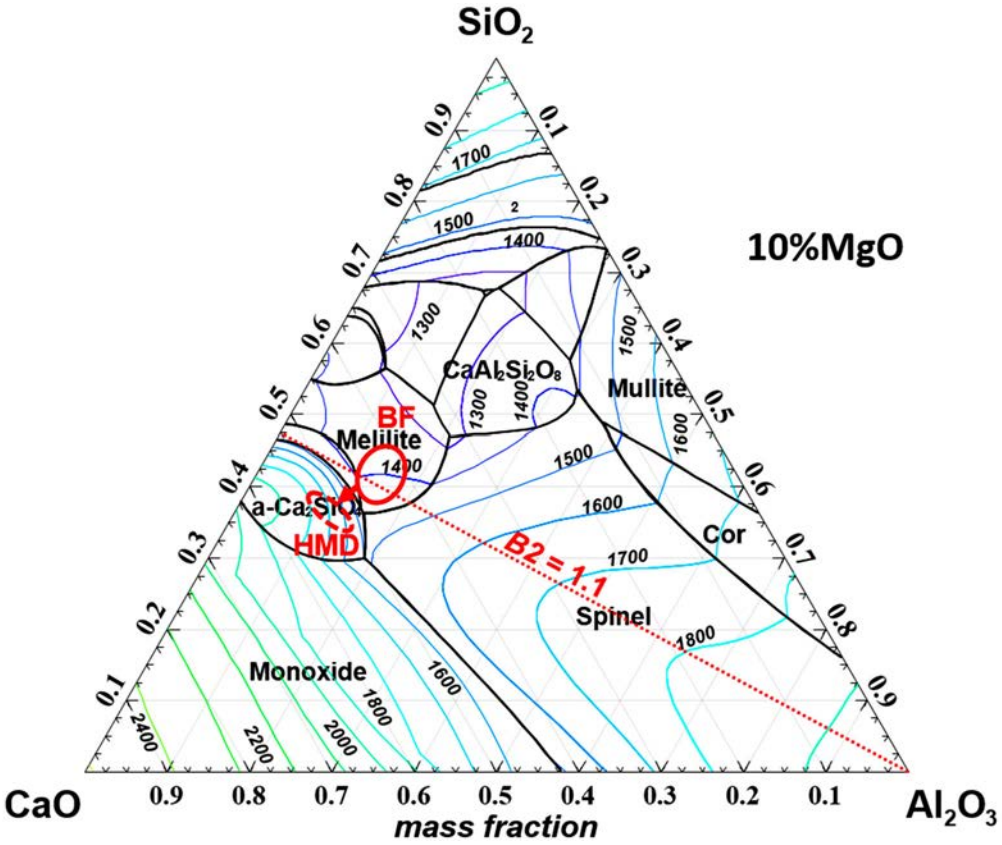

Figure 9. Liquidus projection of CaO-SiO_2-Al_2O_3 slag with 10 wt-% MgO, determined with FactSage. The lines indicate T_{liq} (°C). Typical composition ranges for BF carryover slag ('BF' solid line) and final HMD slag ('HMD' dashed line) are encircled in the diagram. The dotted line indicates where $B2 = 1.1$.

suggest that for a mostly liquid HMD slag MgO should be <10 wt-% and Al_2O_3 should be 12–16 wt-%. The composition range of a typical HMD slag (Table 2) shows that in practice MgO should be as low as possible, while Al_2O_3 should be increased.

Apart from the slag's solid fraction, it has been suggested that the size and shape of the solid particles themselves influence the iron losses as well. Larger and more irregularly shaped slag particles will hamper the settling of the iron droplets in the slag. Magnelöv et al. [7,8,11] showed that addition of the slag modifier nepheline syenite makes the HMD slag look more 'fine-grained' during the HMD process and that this slag was easier to skim. Also cold samples from that slag, after skimming, showed a finer-grained slag compared to the reference slag, with a comparable composition. However, they could not prove that this finer-grained slag actually led to lower iron losses.

Interfacial tension

Interfacial tension is another factor which can influence the iron losses. When the interfacial tension between the slag and the hot metal droplet decreases, it will lead to more friction when metal droplets descend through the slag layer. Therefore, it is expected that a lower interfacial tension will lead to higher iron losses. Interfacial tensions between slag and hot metal are difficult to measure, as slag and hot metal tend to react, thus changing the initial compositions. In general the effect of dissolved elements on the interfacial tension is known [65].

The composition of the hot metal has a larger effect on the interfacial tension than the composition of the slag. Sulphur and oxygen, being surface active elements, have the largest influence on the interfacial tension. More oxygen or sulphur in the hot metal lead to lower interfacial tensions [65]. Therefore, to lower iron losses, the oxygen and sulphur concentration in hot metal should be as low as possible. Given the purpose of the HMD process, the sulphur and oxygen are always kept as low as possible, regardless their effect on the interfacial tension.

Of the elements that lower the interfacial tension of the hot metal, titanium has the largest influence. However, even though a higher titanium content of the hot metal leads to increased iron losses, the effect of the interfacial tension seems to be negligible. The increased iron losses are mostly attributed to the Ti(C,N) formation.

From all typical slag components, FeO and MnO have the largest influence on the interfacial tension. Under HMD conditions, FeO will reduce to Fe and [O], leading to an increased oxygen concentration in the hot metal, which leads to the lower interfacial tension. MnO will react with Fe to form [Mn] and FeO, which on its turn leads to Fe and [O]. Also the effect of other oxides in the slag on the interfacial tension depends on their ability to supply oxygen to the hot metal [65].

Because only little research was done about the effect of interfacial tension on iron losses, as it is difficult to measure [66], there are no reliable figures available on the influence of interfacial tension on iron losses and it is hard to isolate their effect. In general, interfacial tension is not considered as a major factor for iron losses, as iron losses can be explained without it. Furthermore, elements that have the highest influence on the interfacial tension, sulphur and oxygen, are already kept as low as possible in the HMD process. More exotic elements that increase the interfacial tension, like tungsten, are too expensive to use in industry.

Therefore, to find the optimal HMD slag, interfacial tension is not taken into account in this study.

Optimal slag

The optimal HMD slag should be able to contain sufficient sulphur, while leading to the lowest possible iron losses. Under industrial conditions, the sulphur removal capacity of the slag cannot always accurately be predicted by its sulphide capacity (C_S), as the HMD slag is inhomogeneous and as sulphur is also present in the form of solid CaS. However, a comparison between plant data and C_S models shows that C_S can be used to indicate if a certain slag composition is optimal or not. CaO is the most important component in the slag, regarding sulphur removal capacity. There should be enough CaO to react with the sulphur and, based on industrial experience, *B2* (CaO/SiO_2) > 1.1.

To minimise the iron losses with an optimal HMD slag, the focus should be on minimising the colloid losses by lowering η_{slag}. As η_{slag} has an adverse effect on colloid loss and entrainment loss, the focus in industry should be on the colloid loss. At the same time, entrainment loss can be limited by taking other measures like improving skimming skills of operators, improving skimming control or by skimming automation. To lower η_{slag}, both η_0 and $\varphi_{s,slag}$ should be lowered. This can best be done by minimising the MgO content of the slag, preferably < 10 wt-%, and increasing the slag's Al_2O_3 content, preferably 12–16 wt-%. Furthermore, other slag components that lower the η_0 and $\varphi_{s,slag}$, like Na_2O, K_2O and MnO are desirable, keeping in mind that their use can be limited because of other process requirements. The amount of TiO_2 in the slag should be minimised and is ideally 0. For the optimal HMD slag, a *B2* of 1.1 is required, to allow the sulphur removal.

For industry this means that the addition of reagents should be optimised, not only from a desulphurisation point of view, but also to create an optimal slag. Furthermore, a slag modifier could help to further optimise η_{slag}, and thus minimise iron losses.

Conclusions

Based on the fundamentals of hot metal desulphurisation (HMD) slag and industrial data, the following concluding remarks can be made.

- The sulphide capacity (C_S), as defined by Fincham and Richardson [4], is not applicable for direct industrial use, as the industrial slag is inhomogeneous and not necessarily at equilibrium, but C_S can be used to determine the optimal slag composition.
- For a sufficient sulphur removal capacity of the slag, the slag should contain at least enough CaO to allow all MgS to react with CaO to form CaS. Besides, a minimal CaO: SiO_2 weight ratio (*B2*) in the slag of 1.1 is required.
- A lower apparent viscosity of the slag leads to lower overall iron losses.
- Optimising the HMD slag conditions has a higher impact on colloid losses than on entrainment losses. Therefore, in industry, the focus should be on lowering the colloid losses.
- Under industrial circumstances, MgO concentration in the HMD slag should be as low as possible and preferably < 10 wt-%. Al_2O_3 should preferably be 12–16 wt-%.

These remarks on the optimal HMD slag, considering sulphur removal capacity and iron losses, will be validated in part II of this study [12].

List of symbols and abbreviations

Symbols

a_O	Oxygen activity-
B2	Basicity CaO/SiO_2-
C_S	Sulphide capacity –
d_{drop}	Droplet diameterm
f_S	Henrian sulphur activity coefficient –
g	Gravity constant (9.81)$m{\cdot}s^{-2}$
h_{slag}	Slag height m
$K^{\ominus}_{S2}$	Reaction equilibrium constant for reaction 7–
L_S	Sulphur distribution ratio –
n	Constant (typically 2.5)–
p_x	Partial pressure of x Pa
T	Temperature K or °C
T_{liq}	Liquidus temperature K or °C
t_{settle}	Settling times
v_{drop}	Settling speed droplet $m{\cdot}s^{-1}$
X_x	Weight percentage of component xwt-%
α	Maximum solid fraction –
η_0	Viscosity of the liquid fraction of the slagPa·s
η_{slag}	Apparent viscosity of the slag Pa·s
Λ	Optical basicity–
ρ_x	Density of x $kg{\cdot}m^{-3}$
$\varphi_{s,slag}$	Solid volume fraction of the slag-

Abbreviations

BF	Blast furnace
BOF	Basic oxygen furnace, or oxygen steelmaking converter
EMF	Electromagnetic force
HMD	Hot metal desulphurisation
KR	Kanbara reactor
XRF	X-ray fluorescence

Disclosure statement

No potential conflict of interest was reported by the author(s).

ORCID

Frank N. H. Schrama http://orcid.org/0000-0001-9172-4175
Elisabeth M. Beunder http://orcid.org/0000-0001-8734-9261
Jilt Sietsma http://orcid.org/0000-0001-8733-4713
Rob Boom http://orcid.org/0000-0002-0519-0208
Yongxiang Yang http://orcid.org/0000-0003-4584-6918

References

[1] Agricola G. De Re Metallica, Basel (CH), 1556.
[2] Schrama FNH, Beunder EM, van den Berg B, et al. Sulphur removal in ironmaking and oxygen steelmaking. Ironmak Steelmak. 2017;44 (5):333–343. doi:10.1080/03019233.2017.1303914.
[3] Deo B, Boom R. Fundamentals of steelmaking metallurgy, 1st ed. Hemel Hempstead: Prentice-Hall; 1993.
[4] Fincham CJB, Richardson FD. The behaviour of sulphur in silicate and aluminate melts. Proc R Soc London. 1954;223(A):40–62. doi:10.1098/rspa.1954.0099.
[5] Schrama FNH, van den Berg B, Van Hattum G. A comparison of the leading hot metal desulphurization methods. Proceedings of the 6th International Congress on the Science and Technology of Steelmaking, 2015, pp. 61–66.
[6] Schrama FNH, Ji F, Hunt A, et al. Lowering iron losses during slag removal in hot metal desulphurisation without using fluoride. Ironmak Steelmak. 2020;47(5):464–472. doi:10.1080/03019233.2020.1747778.
[7] Magnelöv M, Eriksson J, Drugge J, et al. Investigation of iron losses during desulphurisation of hot metal utilising nepheline syenite.

Ironmak Steelmak. 2013;40(6):436–442. doi:10.1179/1743281212Y.0000000067.
[8] Magnelöv M, Carlsson-Dahlberg A, Gustavsson L, et al. Iron losses during desulphurisation of hot metal utilising co-injection of Mg and CaC_2 combined with nepheline syenite. Ironmak Steelmak. 2015;42(7):525–532. doi:10.1179/1743281214Y.0000000257.
[9] Yang AF, Karasev A, Jönsson PG. Effect of nepheline syenite on iron losses in slags during desulphurization of hot metal. Steel Res Int. 2016;87(5):599–607. doi:10.1002/srin.201500154.
[10] Schrama FNH, Moosavi-Khoonsari E, Beunder EM, et al. Slag optimisation considering iron loss and sulphide capacity in hot metal desulphurisation. Proceedings of the 7th International Congress on the Science and Technology of Steelmaking, 2018, p. ICS131.
[11] Magnelöv M. Iron losses during desulphurisation of Hot Metal, (PhD thesis) Luleå University of Technology, Luleå (SE), 2014.
[12] Schrama FNH, Beunder EM, Panda SK, et al. Optimal hot metal desulphurisation slag considering iron loss and sulphur removal capacity part II: Validation. Ironmak Steelmak. 2021. doi: 10.1080/03019233.2021.1882648
[13] Bale CW, Chartrand P, Degterov SA, et al. Factsage thermochemical software and databases, 2010-2016. Calphad Comput Coupling Phase Diagrams Thermochem. 2016;54:35–53. doi:10.1016/j.calphad.2016.05.002.
[14] Visser H-J. "Modelling of injection processes in ladle metallurgy," (PhD thesis) Delft University of Technology, Delft (NL), 2016.
[15] Kitamura S. Hot metal Pretreatment. In: S Seetharaman, editor. *Treatise on process metallurgy*, vol. 3. Oxford: Elsevier; 2014. p. 177–221.
[16] Yang Y, Raipala K, Holappa L. Ironmaking. In: S Seetharaman, editor. Treatise on process metallurgy, vol. 3. Oxford: Elsevier; 2014. p. 2–88.
[17] Geerdes M, Chaigneau R, Kurunov I, et al. Modern blast furnace ironmaking, 3rd ed. Delft (NL): IOS Press; 2015.
[18] Holappa L. Secondary steelmaking, 1st ed., vol. 3. Oxford: Elsevier Ltd.; 2014.
[19] Zhang G, Wang N, Chen M, et al. Viscosity and Structure of CaO–SiO_2–'FeO'–$Al2O_3$–MgO system during iron-extracting process from nickel slag by Aluminum Dross. Part 1: coupling effect of 'FeO' and $Al2O_3$. Steel Res Int. 2018;89:1800272, doi:10.1002/srin.201800272.
[20] CRCT (Canada) & GTT (Germany). FactSage 7.3, 2020. [Online]. Available: www.factsage.com.
[21] Gavel DJ. Shifting the limits of nut coke use in the ironmaking blast furnace, (PhD thesis) Delft University of Technology, Delft (NL), 2020.
[22] Freißmuth A. Die Entschwefelung von Roheisen, 1st ed. Tisnov (CZ): Almamet GmbH; 2004.
[23] Janke D. Metallurgische Sensortechnik. In: Electrochemische Sauerstoffmessung in der Metallurgie, 1st ed. Düsseldorf, DE: Verlag Stahleisen; 1985. p. S 216–S 222.
[24] Moosavi-Khoonsari E, Jung IH. Thermodynamic modeling of sulfide capacity of Na_2O-containing oxide melts. Metall Mater Trans B. 2016;47(5):2875–2888. doi:10.1007/s11663-016-0749-z.
[25] Hino M, Kitagawa S, Ban-ya S. Sulphide capacities of CaO-Al_2O_3-SiO_2 and CaO-Al_2O_3-MgO slags. ISIJ Int. 1993;33(1):36–42.
[26] Panda SK, Harbers E, Overbosch A, et al. Desulphurization with ladle furnace slag). Proceedings of METEC & 4th ESTAD, 2019.
[27] Yang X, Jiao J, Ding R, et al. A thermodynamic model for calculating sulphur distribution ratio between CaO-SiO_2 -MgO-Al_2O_3 ironmaking slags and carbon saturated hot metal based on the Ion and molecule coexistence theory. ISIJ Int. 2009;49(12):1828–1837. doi:10.2355/isijinternational.49.1828.
[28] Shi C-B, Yang X-M, Jiao J-S, et al. A sulphide capacity prediction model of CaO-SiO_2-MgO-Al_2O_3 ironmaking slags based on the ion and molecule coexistence theory. ISIJ Int. 2010;50(10):1362–1372. doi:10.2355/isijinternational.50.1362.
[29] Ender A, Van Den Boom H, Kwast H, et al. Metallurgical development in steel-plant-internal multi-injection hot metal desulphurisation. Steel Res Int. 2005;76(8):562–572.
[30] Zhao Y, Irons GA. The role of oxygen in hot metal desulphurization with calcium carbide. Scaninject V - Part II. 1989: 63–81.
[31] Mampaey F, Habets D, Plessers J, et al. On line oxygen activity measurements to determine optimal graphite form during compacted graphite iron production. Int J Met. 2010;4(2):25–43.
[32] Mampaey F, Habets D, Seutens F. The use of oxygen activity measurement to determine optimal properties of ductile iron during production. Int Foundry Res. 2008;60(1):2–19.
[33] Schrama FNH, Beunder EM, Visser H-J, et al. The Hampering effect of precipitated carbon on hot metal desulfurization with magnesium. Steel Res Int. 2019: 201900441, doi:10.1002/srin.201900441.
[34] Jung IH, Moosavi-Khoonsari E. Limitation of sulfide capacity concept for molten slags. Metall Mater Trans B. 2016;47(2):819–823. doi:10.1007/s11663-016-0594-0.
[35] Duffy JA, Ingram MD. Establishment of an optical scale for Lewis basicity in inorganic oxyacids, molten salts, and glasses. J Am Chem Soc. 1971;93(24):6448–6454. doi:10.1021/ja00753a019.
[36] Young RW. Use of optical basicity concept for determining phosphorus and sulphur slag–metal partitions, (EUR 13176 EN) Luxembourg, 1991.
[37] Young RW, Duffy JA, Hassal GJ, et al. Use of the optical basicity concept for determining phosphorus and sulphur slag-metal partitions. Ironmak Steelmak. 1992;19(3):201–219.
[38] Ma X, Chen M, Xu H, et al. Sulphide capacity of CaO-SiO_2-Al_2O_3-MgO system relevant to low MgO blast furnace slags. ISIJ Int. 2016;56(12):2126–2131. doi:10.2355/isijinternational.ISIJINT-2016-274.
[39] Condo AFT, Qifeng S, Sichen D. Sulfide capacities in the Al_2O_3-CaO-MgO-SiO_2 system. Steel Res Int. 2018;89:1800061), doi:10.1002/srin.201800061.
[40] Taniguchi Y, Sano N, Seetharaman S. Sulphide capacities of CaO–Al_2O_3–SiO_2–MgO–MnO slags in the temperature range 1673–1773K. ISIJ Int. 2009;49(2):156–163.
[41] Hao X, Wang X. A new sulfide capacity model for CaO-Al_2O_3-SiO_2-MgO slags based on corrected optical basicity. Steel Res Int. 2016;87(3):359–363. doi:10.1002/srin.201500065.
[42] Shankar A, Görnerup M, Lahiri AK, et al. Sulfide capacity of high alumina blast furnace slags. Metall Mater Trans B. 2006;37B:941–947.
[43] Sosinsky DJ, Duffy JA. The composition and temperature dependence of the sulfide capacity of metallurgical slags. Metall Mater Trans B. 1986;17(2):331–337.
[44] Zhang G-H, Chou K-C, Pal U. Estimation of sulfide capacities of multicomponent slags using optical basicity. ISIJ Int. 2013;53(5):761–767. doi:10.2355/isijinternational.53.761.
[45] Condo AFT, Allertz C, Sichen D. Experimental determination of sulphide capacities of blast furnace slags with higher MgO contents. Ironmak Steelmak. 2019;46(3):207–210. doi:10.1080/03019233.2017.1366089.
[46] Andersson MAT, Jönsson PG, Hallberg M. Optimisation of ladle slag composition by application of sulphide capacity model. Ironmak Steelmak. 2000;27(4):286–293. doi:10.1179/030192300677570.
[47] Nzotta MM, Andreasson M, Jo P. A study on the sulphide capacities of steelmaking slags. Scand J Metall. 2000;29(2):177–184. doi:10.1034/j.1600-0692.2000.d01-21.x.
[48] Chatterjee S, Konar B, Maity A, et al. Development of alternative flux for liquid steel desulfurization. AISTech 2019 – Proceedings of the Iron & Steel Technology Conference, 2019, pp. 1211–1224, doi:10.33313/377/123.
[49] Schrama FNH, Beunder EM, Ji F, et al. Effect of KAlF4 on the efficiency of hot metal desulphurisation with magnesium. European Oxygen Steelmaking Conference (EOSC), 2018, p. EOSC021.
[50] Brooks GA, Hasan MM, Rhamdhani MA. Slag basicity: what does it Mean?. 10th International Symposium on High-Temperature Metallurgical Processing, 2019, pp. 297–308, doi:10.1007/978-3-030-05955-2_28.
[51] Turkdogan ET. Fundamentals of steelmaking. London: The Institute of Materials; 1996.
[52] Li Z, van Boggelen JWK, Thomson H, et al. Improved slag skimming performance at hot metal desulphurisation station by using recycled materials as slag modifying agent. Scanmet IV. 2012: 189–195.
[53] Yang AF, Karasev A, Jönsson PG. Characterization of metal droplets in slag after desulfurization of hot metal. ISIJ Int. 2015;55(3):570–577. doi:10.2355/isijinternational.55.570.
[54] Yang AF, Karasev A, Jonsson PG. Behavior of metal droplets in slags during desulphurization of hot metal. Proceedings of the 6th International Congress on the Science and Technology of Steelmaking, ICS 2015, 2015, pp. 80–83.
[55] Iwamasa PK, Fruehan RJ. Separation of metal droplets from slag. ISIJ Int 1996;36(11):1319–1327.
[56] Diao J, Xie B, Wang SS. Research on slag modifying agents for CaO–Mg based hot metal desulphurisation. Ironmak. Steelmak. 2009;36(7):543–547. doi:10.1179/174328109X445642.

[57] Han Z, Holappa L. Mechanisms of iron entrainment into slag due to rising gas bubbles. ISIJ Int. 2003;43(3):292–297. doi:10.2355/isijinternational.43.292.
[58] Roscoe R. The viscosity of suspension of rigid spheres. Br J Appl Phys. 1952;3:267–269.
[59] Mills KC, Sridhar S. Viscosities of ironmaking and steelmaking slags. Ironmak Steelmak. 1999;26(4):262–268. doi:10.1179/030192399677121.
[60] Li Z, Bugdol M, Crama W. "Optimisation of hot metal desulphurisation slag in the CaO / Mg co-injection process to improve slag skimming performance," in *Molten 2012*, 2012.
[61] Wu L, Ek M, Song M, et al. The effect of solid particles on liquid viscosity. Steel Res Int. 2011;82(4):388–397. doi:10.1002/srin.201000207.
[62] Wang C, Zhang J, Jiao K, et al. Influence of basicity and MgO/Al_2O_3 ratio on the viscosity of blast furnace slags containing chloride. Metall Res Technol. 2017;114(2):205), doi:10.1051/metal/2016064.
[63] Park H, Park JY, Kim GH, et al. Effect of TiO_2 on the viscosity and slag structure in blast furnace type slags. Steel Res Int. 2012;83(2):150–156. doi:10.1002/srin.201100249.
[64] Street S, Stone RP, Koros PJ. The presence of titanium in hot metal and its effects on desulfurization. Iron Steel Technol. 2005;2(11):65–74.
[65] Nakashima K, Mori K. Interfacial properties of liquid iron alloys and liquid slags relating to iron- and steel-making processes. ISIJ Int. 1992;32(1):11–18. doi:10.2355/isijinternational.32.11.
[66] Miedema AR, Boom R. Surface tension and electron density of pure liquid metals. Zeitschrift Fuer Met Res Adv Tech. 1978;69(3):183–190.